



RESEARCH ARTICLE

Hydrological regulation of chemical weathering and dissolved inorganic carbon biogeochemical processes in a monsoonal river

Jing Liu¹  | Jun Zhong^{2,3}  | Hu Ding^{3,4} | Fu-Jun Yue⁴ | Cai Li^{2,5} | Sen Xu² | Si-Liang Li²

¹School of Management Science, Guizhou University of Finance and Economic, Guiyang, China

²Institute of Surface-Earth System Science, Tianjin University, Tianjin, China

³The State Key Laboratory of Environmental Geochemistry, Institute of Geochemistry, Chinese Academy of Sciences, Guiyang, China

⁴School of Geographical and Earth Sciences, University of Glasgow, Glasgow, UK

⁵School of Urban and Environment Science, Huaiyin Normal University, Huaian, China

Correspondence

Jun Zhong, Institute of Surface-Earth System Science, Tianjin University, Tianjin 300073, China.

Email: jun.zhong@tju.edu.cn

Funding information

Guizhou Education Department Fund, Grant/Award Number: [2018]161; Guizhou Science and Technology Department Fund, Grant/Award Number: [2019]1043; National Key R&D Program of China, Grant/Award Number: 2016YFA0601002; National Natural Science Foundation of China, Grant/Award Numbers: 41422303, 41571130072; Guizhou University of Finance and Economics, Grant/Award Number: [2018]5774-029

Abstract

To better understand the mechanisms relating to hydrological regulations of chemical weathering processes and dissolved inorganic carbon (DIC) behaviours, high-frequency sampling campaigns and associated analyses were conducted in the Yu River, South China. Hydrological variability modifies the biogeochemical processes of dissolved solutes, so major ions display different behaviours in response to discharge change. Most ions become diluted with increasing discharge because of the shortened reactive time between rock and water under high-flow conditions. Carbonate weathering is the main source of major ions, which shows strong chemostatic behaviour in response to changes in discharge. Ions from silicate weathering exhibit a significant dilution effect relative to the carbonate-sourced ions. Under high temperatures, the increased soil CO₂ influx from the mineralisation of organic material shifts the negative carbon isotope ratios of DIC ($\delta^{13}\text{C}_{\text{DIC}}$) during the high-flow season. The $\delta^{13}\text{C}_{\text{DIC}}$ values show a higher sensitivity than DIC contents in response to various hydrological conditions. Results from a modified isotope-mixing model (*IsoSource*) demonstrate that biological carbon is a dominant source of DIC and plays an important role in temporal carbon dynamics. Furthermore, this study provides insights into chemical weathering processes and carbon dynamics, highlighting the significant influence of hydrological variability to aid understanding of the global carbon cycle.

KEYWORDS

carbon isotope, chemical weathering processes, DIC dynamics, hydrological variability, karst, monsoonal river

1 | INTRODUCTION

Rivers are primary conduits transporting terrestrial weathering loads from continents to the ocean (Li & Bush, 2015; McClanahan, Polk, Groves, Osterhoudt, & Grubbs, 2016; Schulte et al., 2011). In addition, chemical weathering is the main source of dissolved loads in rivers, which removes large amounts of atmospheric CO₂ and plays a critical role in the global carbon cycle (Clow & Mast, 2010; Gaillardet, Dupré, Louvat, & Allègre, 1999; Zhong et al., 2018). Carbonate dissolution

consumes nearly 12.3×10^{12} mol of carbon per year and is an important carbon sink in short-term carbon balance (Gaillardet et al., 1999). Previous studies have established that hydrological processes govern riverine solute transport and carbon cycling by affecting biogeochemical reactions (Maher & Chamberlain, 2014; Zhong et al., 2018). Furthermore, the chemical weathering processes can be altered easily through changing hydrological conditions (Gareis & Lesack, 2017; Torres, West, & Clark, 2015; Zhong et al., 2018). Although numerous studies of chemical weathering and CO₂ consumption rate have been

carried out on rivers worldwide (Amiotte Suchet, Probst, & Ludwig, 2003; Gaillardet et al., 1999; Galy & France-Lanord, 1999; Krishna, Viswanadham, Prasad, Kumari, & Sarma, 2018; Li et al., 2010; Li, Calmels, Han, Gaillardet, & Liu, 2008; Louvat & Allègre, 1997; Millot, Gaillardet, Dupré, & Allègre, 2002; Ollivier, Hamelin, & Radakovitch, 2010; Rai, Singh, & Krishnaswami, 2010; Roy, Gaillardet, & Allegre, 1999), few were devoted to temporal chemical weathering processes, and fewer still focused on the effects of hydrological variability on chemical weathering processes in monsoonal rivers.

It has been estimated that rivers transfer approximately 1 Gt of carbon annually to the ocean (Amiotte Suchet et al., 2003; Li & Bush, 2015). Moreover, riverine dissolved inorganic carbon (DIC) transports 38% of the total carbon from continents to the ocean, which is a much higher proportion in the Xijiang River, at 80% (Zhong et al., 2018). Accordingly, DIC dynamics in carbonate-rich rivers play an important role in the regional and even the global carbon cycle (Zhong et al., 2018). However, global carbon budgets and biogeochemical processes are inadequately restricted by the variability in hydrological conditions (Li et al., 2010; Raymond & Cole, 2003; Zhong, Li, Tao, Ding, & Liu, 2017). Riverine DIC is controlled by water-gas exchange, plant photosynthesis/respiration, and mineral weathering (Bouillon et al., 2014; Brunet et al., 2009; Doctor et al., 2008; McClanahan et al., 2016; Raymond & Cole, 2003; Tobias & Böhlke, 2011; Zhong, Li, Tao, Ding, & Liu, 2017), all of which are significantly influenced by hydrological variability. To distinguish riverine DIC sources and relative biogeochemical processes under various hydrological conditions, carbon isotope ratios of DIC ($\delta^{13}\text{C}_{\text{DIC}}$) can be a useful tool (Cerling, Solomon, Quade, & Bowman, 1991; Clark & Fritz, 1997; Dubois, Lee, & Veizer, 2010; Li et al., 2010; McClanahan et al., 2016; Zhong, Li, Tao, Ding, & Liu, 2017). However, the underlying biogeochemical processes under various hydrological conditions are poorly understood, and the relative response mechanisms of carbon dynamics to hydrological variability remain unknown.

The Yu River located in one of the largest carbonate outcrop areas (approximately 90,000 km²; Jiang, Liu, Zhao, Sun, & Xu, 2018) in China, and it is also one of the largest rivers in Guangxi to be affected by monsoon climate. It is ideal for investigations of chemical weathering processes and the response of riverine DIC dynamics to hydrological variability. In the present study, time-series sampling procedures and analyses were performed to (a) understand chemical weathering processes under various hydrological conditions, (b) identify DIC sources, and (c) distinguish the underlying carbon biogeochemical processes under conditions of hydrological variability.

2 | METHODS

2.1 | Study area

The Yu River catchment lies in the southern margin of the Southeast Asian Karst Region (Jiang et al., 2018; Xu & Liu, 2010). It is the largest tributary on the south bank of the Xijiang River, the mainstream of the

Pearl River (Figure 1). The drainage area of the Yu River is 89,870 km², with a mean annual precipitation of 1,500–2,000 mm. The Yu River catchment experiences a humid subtropical climate under monsoonal conditions, resulting in high precipitation in summer and low precipitation in winter. Lithologically, the hinterland ranges from Precambrian metamorphic rocks to Quaternary fluvial sediments. Carbonate rocks (limestone and dolomite) are widely distributed in this area (Yuan, 1991), as well as occasional evaporate outcrops (Geological Bureau of Guangxi Zhuang Autonomous Region, 1985). Furthermore, sedimentary rocks and coal-bearing formations are widely distributed in the study area, and the coal deposits are rich in sulphides (Gao et al., 2009; Li et al., 2008; Xu & Liu, 2010). Igneous rocks are mainly distributed in the eastern part of the Yu River catchment (Geological Bureau of Guangxi Zhuang Autonomous Region, 1985).

2.2 | Sample collection and laboratory analysis

The sampling site was located at the outlet of the Yu River catchment (Figure 1), approximately 26 km from the mainstream of the Xijiang River. Water samples for hydrochemical and isotopic analyses were collected monthly from October 2013 to September 2014. Additional samples were collected in the high-flow season based on changes in discharge (Figure 2). The alkalinity of samples was determined using 0.02-M HCl titration within 24 hr of collection. After filtration through 0.45- μM cellulose-acetate membrane paper, the anions (Cl^- , SO_4^{2-} , and NO_3^-) were determined using the Dionex Ion Chromatography System 90 (Sunnyvale, CA) within a relative standard deviation (RSD) of 5%. The major cations (K^+ , Na^+ , Ca^{2+} , and Mg^{2+}) and dissolved Si were determined by inductively coupled plasma-optical emission spectrometry, within an RSD of 3%, after acidification to pH ≤ 2 . The samples used for $\delta^{13}\text{C}_{\text{DIC}}$ analyses were collected in polyethylene bottles with airtight caps. Using a modified version of the method described by Li et al. (2010), 15 ml aliquots of the samples were injected with syringes into glass bottles that were previously loaded with 2 ml of 85% phosphoric acid and magnetic stirrer bars. CO_2 was extracted via a vacuum line and transferred cryogenically into a tube for isotope measurement. In addition, the carbon isotopic ratios were determined using a Finnigan MAT 252 mass spectrometer and are reported in the δ -notation relative to the Vienna Pee Dee Belemnite scale as per mil with a precision of 0.1%. All the analyses were conducted at the State Key Laboratory of Environmental Geochemistry, Institute of Geochemistry, Chinese Academy of Sciences.

Daily hydrological data including water discharge (m³/s), precipitation (mm), water temperature ($^{\circ}\text{C}$), water surface evaporation (mm), suspended sediment load (kg/s), and water level (m) were obtained from the Hydrological Yearbook (Pearl River Conservancy Committee, 2013) produced by the Pearl River Conservancy Commission. We used LoadRunner software (Booth, Raymond, & Oh, 2007) in the USGS LOADEST program (Runkel, Crawford, & Cohn, 2004) to model the dissolved solute contents and carbon isotopic values. A mixing model, *IsoSource*, was employed to predict the specific riverine DIC source contributions.

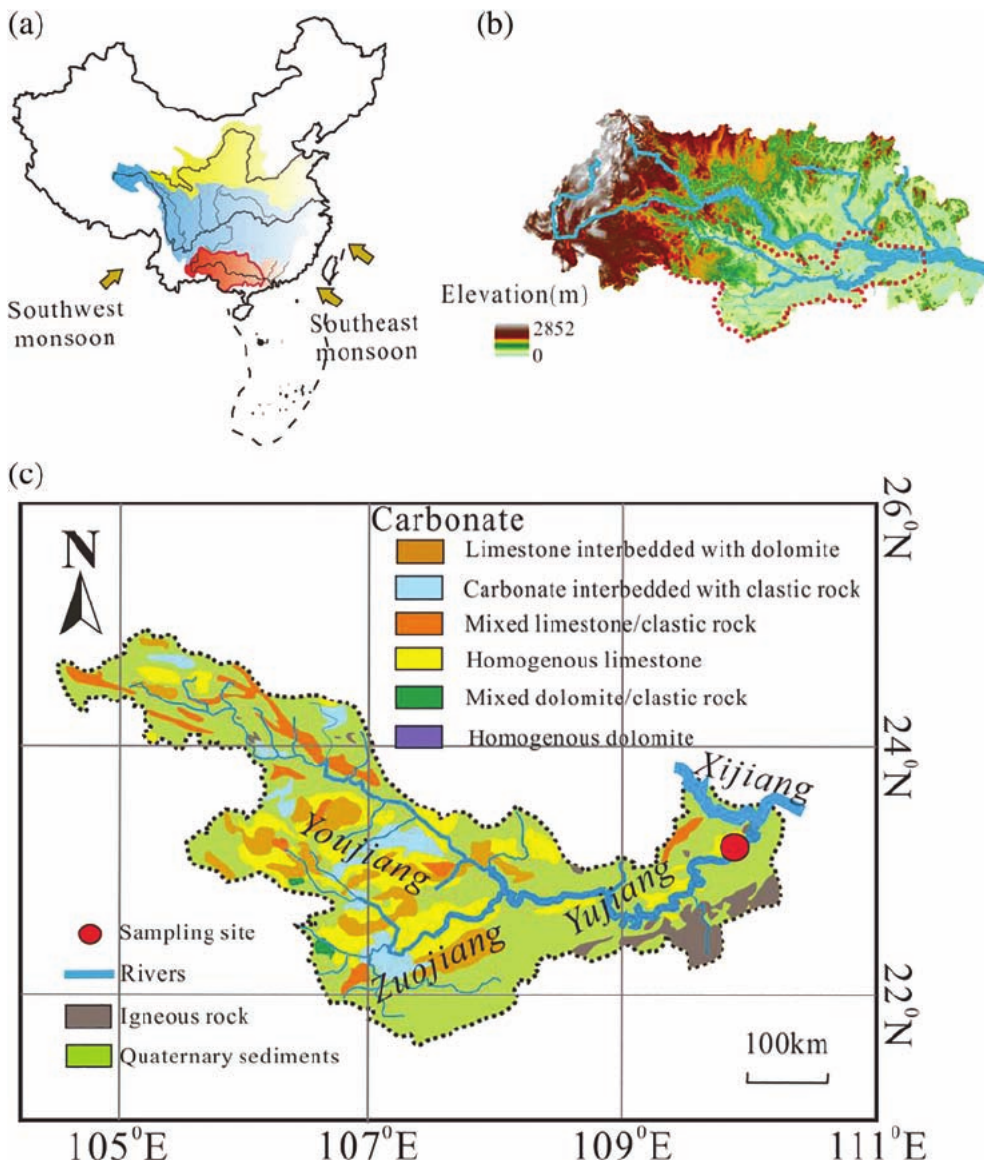


FIGURE 1 Map showing the sampling location and the geological background of the Yu River catchment (c), which is the largest tributary on the south bank of the Xijiang River (b), south China (a)

3 | RESULTS

3.1 | Temporal variations of hydrological parameters

For the Yu River, the discharge was low in October 2013, peaked in November, then dropped quickly and stabilized at a minimum value from January to April 2014. The fluctuating discharge occurred in the high-flow season and reached another peak in August 2014. The water level varied with the changing discharge levels, which fluctuated in the high-flow season and were relatively stable in the low-flow season. The water temperature records for the Yu River indicated that seasonal trends follow meteorological trends. The highest water temperature was 31°C for the hydrological year, which corresponded to high water surface evaporation, while in the low-flow season, as the water temperature decreased, the water surface evaporation decreased accordingly. The total suspended sediment load also showed three peaks corresponding to the discharge variation.

3.2 | Characteristics of major ions and carbon isotopes

The riverine water was mildly alkaline, so HCO_3^- was the major inorganic carbon species (Clark & Fritz, 1997; Hélie, Hillaire-Marcel, & Rondeau, 2002; Zhong et al., 2018). The electrical conductivity values varied from 177 to 325 $\mu\text{S}/\text{cm}$. The total cationic charge ($\text{TZ}^+ = \text{K}^+ + \text{Na}^+ + 2\text{Ca}^{2+} + 2\text{Mg}^{2+}$) and total dissolved anionic charge ($\text{TZ}^- = \text{HCO}_3^- + \text{Cl}^- + \text{NO}_3^- + 2\text{SO}_4^{2-}$) were well balanced, for all normalized ionic charge balance (NICB) values: $\text{NICB} = (\text{TZ}^+ - \text{TZ}^-) \times 100\% / (\text{TZ}^+ + \text{TZ}^-)$, within $\pm 5\%$. The total dissolved solids ($\text{TDS} = \text{K}^+ + \text{Na}^+ + \text{Ca}^{2+} + \text{Mg}^{2+} + \text{HCO}_3^- + \text{Cl}^- + \text{NO}_3^- + \text{SO}_4^{2-} + \text{SiO}_2$, mg/L) ranged from 170 to 254 mg/L , with an average of 211 mg/L , higher than the world average value (97 mg/L ; Li & Bush, 2015). The base cation content ranges were 824–1,245 $\mu\text{mol}/\text{L}$ for Ca^{2+} , 110–232 $\mu\text{mol}/\text{L}$ for Mg^{2+} , 77–287 $\mu\text{mol}/\text{L}$ for Na^+ , and 39–77 $\mu\text{mol}/\text{L}$ for K^+ . The major anion content ranges were 1,731–2,574 $\mu\text{mol}/\text{L}$ for HCO_3^- , 96–203 $\mu\text{mol}/\text{L}$ for SO_4^{2-} , 85–285 $\mu\text{mol}/\text{L}$ for Cl^- , and 19–150 $\mu\text{mol}/\text{L}$ for NO_3^- . Most of

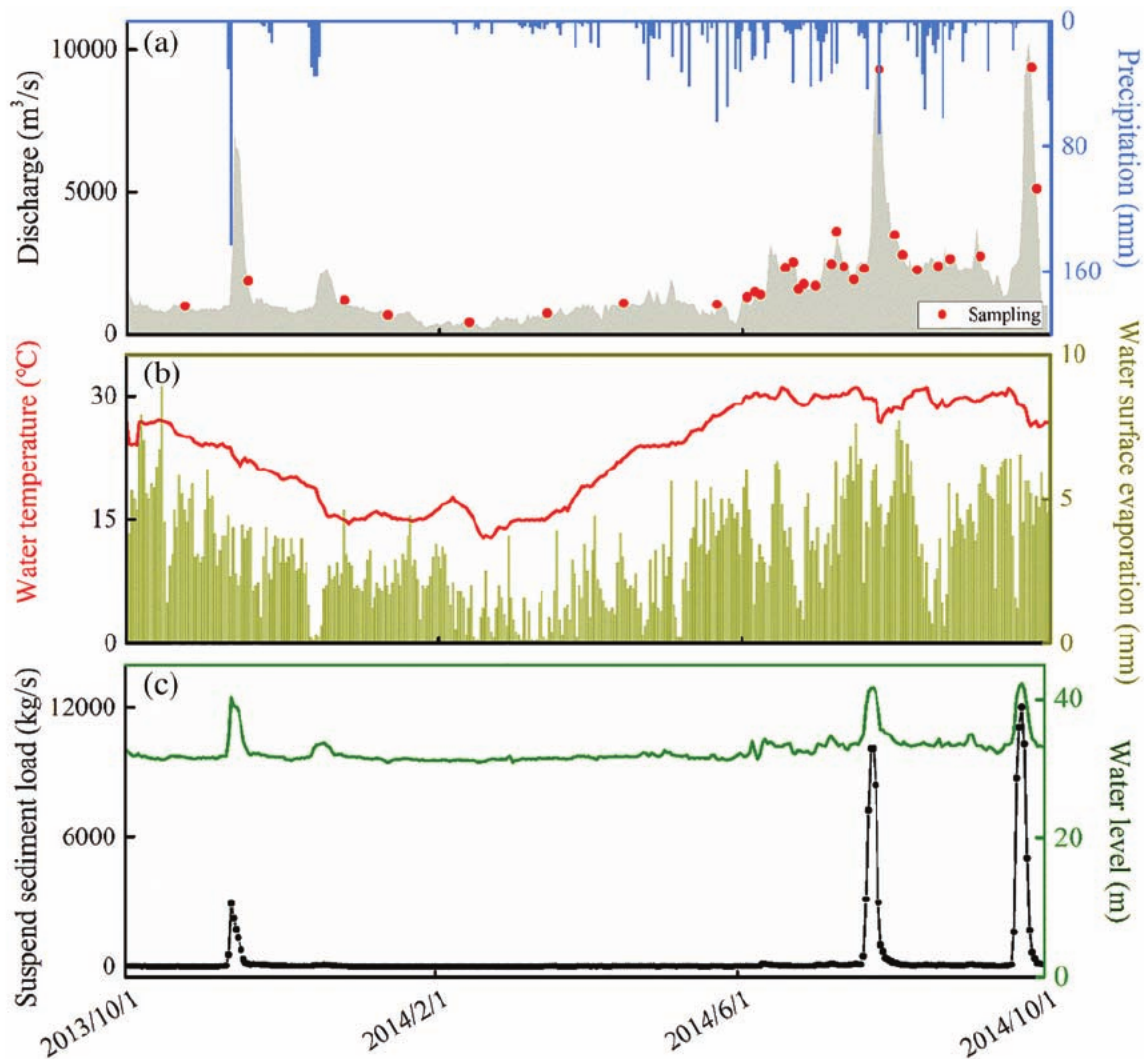


FIGURE 2 Hydrological parameters in the Yu River during the sampling period, discharge and precipitation (a); water temperature and water surface evaporation (b); suspended sediment load and water level (c) for the hydrological year

the major ions show distinct temporal variations during the hydrological year, with high content in the low-flow seasons and low content in the high-flow seasons. However, for NO_3^- , which may be affected by multiple biological processes, no clear temporal variations were discovered during the study period. The riverine water had high contents of Ca^{2+} , Mg^{2+} , and HCO_3^- , consistent with the typical characteristics of carbonate-dominated rivers (Hélie et al., 2002; Jiang et al., 2018; Li et al., 2008; Zhong, Li, Tao, Ding, & Liu, 2017). The $\delta^{13}\text{C}_{\text{DIC}}$ values ranged from -14.6 to -9.6% , with an average value of -12.8% , showing distinct temporal variations.

4 | DISCUSSION

4.1 | Controls on concentration–discharge (C-Q) relationship

Numerous studies have demonstrated that most dissolved solute concentrations negatively correlate with discharge, which can be

represented as a power-law function (Ali et al., 2017; Clow & Mast, 2010; Diamond & Cohen, 2018; Godsey, Kirchner, & Clow, 2009; Gwenzi, Chinyama, & Togarepi, 2017; Kim, Dietrich, Thurnhoffer, Bishop, & Fung, 2017; Koger, Newman, & Goering, 2018; Musolff, Schmidt, Selle, & Fleckenstein, 2015; Rose, Karwan, & Godsey, 2018; Rue et al., 2017; Singley et al., 2017):

$$C = a \times Q^b, \quad (1)$$

where a is a constant, and b reflects the index of the deviation from chemostatic behaviour (Clow & Mast, 2010). When b is close to 0, there is a weak relationship between solute concentrations and discharge, implying chemostatic behaviour (Godsey et al., 2009); when $b > 0$, solute concentrations increase with increasing discharge (Musolff et al., 2015); however, when $b = -1$, the solute contents decrease with increasing discharge, when Q is the only control on C (Godsey et al., 2009). The C-Q relationships of Ca^{2+} , Mg^{2+} , HCO_3^- , K^+ , and SO_4^{2-} display more significant chemostatic behaviour than that of Na^+ and Cl^- (Figure 3), which show a significant dilution effect

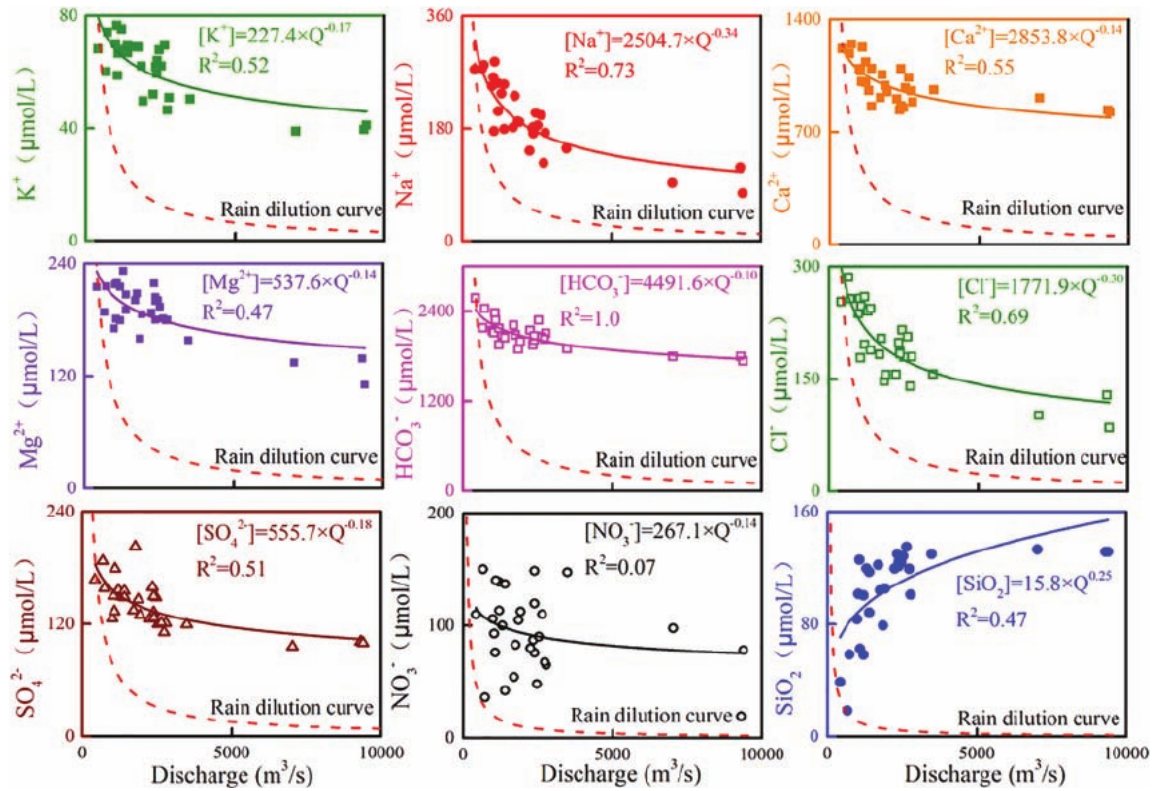


FIGURE 3 the concentration-discharge relationships of dissolved solutes (K^+ , Na^+ , Ca^{2+} , Mg^{2+} , HCO_3^- , Cl^- , NO_3^- , SO_4^{2-} and Si) for the Yu River

caused by rainwater. However, the dissolved Si concentrations have a positive power-law relationship with Q (Figure 3).

The coefficients of variations of the solute concentrations and discharge (CV_C/CV_Q) facilitate an understanding of the behaviour of solute concentrations in response to hydrological variability (Musolff et al., 2015; Thompson, Basu, Lascrain, Aubeneau, & Rao, 2011), which is expressed as:

$$CV_C/CV_Q = (\mu_Q \sigma_C) / (\mu_C \sigma_Q), \quad (2)$$

where μ_C and μ_Q are the average values of the concentrations and discharge, and σ_C and σ_Q are the standard deviations of the concentrations and discharge, respectively (Zhong et al., 2018). Chemostatic behaviour was defined as $-0.2 < b < 0.2$ and $CV_C/CV_Q < 0.5$ based on the methodology of Musolff et al. (2015). Chemodynamic behaviour ($b \approx 0$, $CV_C/CV_Q > 1$) is discharge-independent; therefore, dissolved solute concentrations are independent of Q (Musolff et al., 2015; Zhong et al., 2018). The Ca^{2+} , Mg^{2+} , and HCO_3^- concentrations from the Yu River fall into the same range as those in the Xijiang River (Figure 4), representing near-chemostatic behaviour (Zhong et al., 2018) that can be ascribed to fast carbonate dissolution and precipitation kinetics (Tipper et al., 2006; Zhong et al., 2018; Zhong, Li, Tao, Ding, & Liu, 2017). Silicate weathering is the main source of Na^+ ; it shows a significant dilution effect implying that solutes from silicate weathering are more sensitive to hydrological change. SO_4^{2-} might be derived from various sources,

such as gypsum dissolution, sulphide oxidation, and anthropogenic inputs. Moreover, sulphuric acid has been proved to play an important role in carbonate weathering in South China (Li et al., 2008; Liu et al., 2017). However, although NO_3^- yields high CV_C/CV_Q ratios and near-zero b values, presenting chemostatic behaviour, it shows a chemodynamic pattern. The near-chemodynamic behaviour correlates with the transformations of soil organic nitrogen and nitrification and denitrification reactions under various hydrological processes (Koger et al., 2018).

4.2 | Sources of dissolved solutes

Riverine-dissolved solutes are derived mainly from rock weathering, atmospheric, and human inputs (Gaillardet et al., 1999; Han & Liu, 2004; Zhong et al., 2018). The fast dissolution kinetic of carbonate rocks means that carbonate weathering plays a significant role in the water chemistry of most global rivers, particularly in South China (Gaillardet et al., 1999; Li et al., 2008; Zhong et al., 2018; Zhong, Li, Tao, Ding, & Liu, 2017). The sum of Ca^{2+} and HCO_3^- accounts for 77% of the total ions in the Yu River, demonstrating the dominant contribution of carbonate weathering to local water chemistry, which is similar to the results of previous studies (Jiang et al., 2018; Xu & Liu, 2010). The relationship between Ca^{2+}/Na^+ ratios and Mg^{2+}/Na^+ ratios yields a strong linear correlation over the hydrological year, and the ratios of Ca^{2+}/Na^+ and Mg^{2+}/Na^+ in the high-flow season are

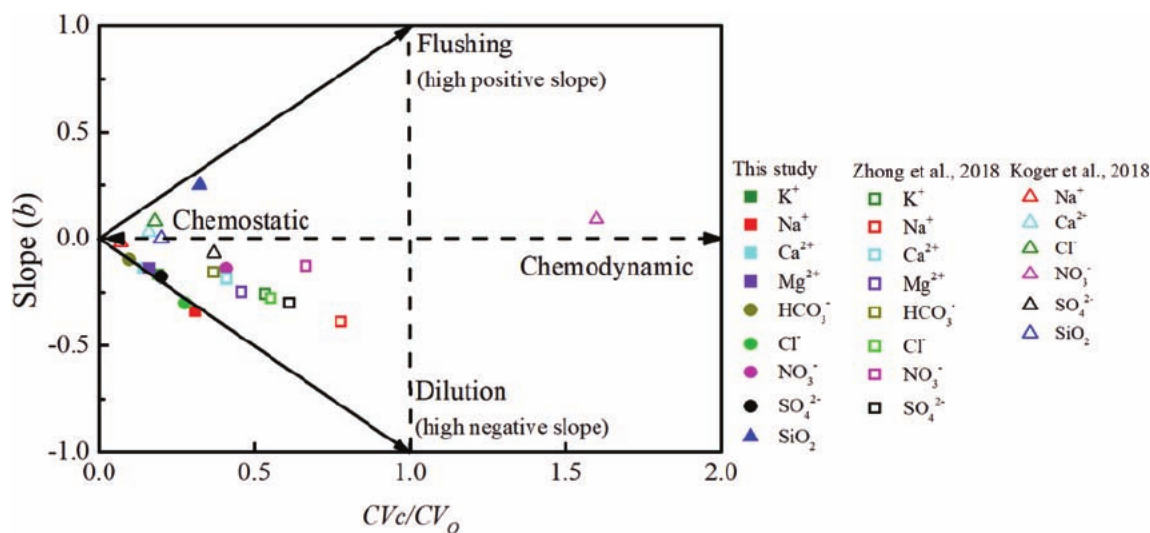


FIGURE 4 Plot of slope (b) versus CV_c/CV_0 for dissolved solutes of the Yu River, the Xijiang River (Zhong et al., 2018) and the Cañon de Valle River (Koger et al., 2018)

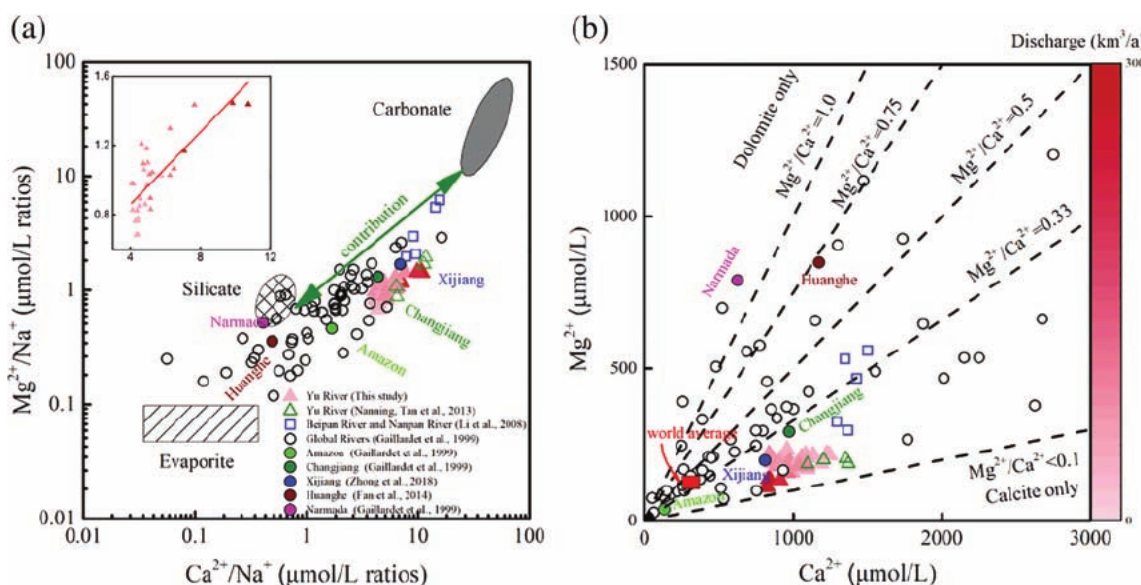


FIGURE 5 The relationships between Ca^{2+}/Na^+ and Mg^{2+}/Na^+ (a), the correlation of Ca^{2+} versus Mg^{2+} (b) in the Yu River, compared with global rivers

much higher than those in the low-flow season (Figure 5a). The ratio of Mg^{2+}/Ca^{2+} represents the relative contribution of dolomite and calcite, as Mg^{2+} is mainly derived from dolomite. As shown in Figure 5b, a ratio of <0.1 represents calcite only; a ratio equal to 1 indicates dolomite dominance; and a ratio of ≈ 0.33 indicates a roughly equal contribution from calcite and dolomite weathering (Szramek et al., 2007). For the Yu River, the ratio of Mg^{2+}/Ca^{2+} generally exceeds the value of 0.1 but is less than 0.33. This indicates that carbonate weathering ions are mainly derived from calcite weathering, particularly in the high-flow season; this result is consistent with previous studies (Jiang et al., 2018). In the high-flow season, high temperature accelerates the solubility of calcite, with ratios indicating a

higher rate of the former than that of dolomite (Schulte et al., 2011; Szramek et al., 2007).

4.3 | Impacts of climatic variability on chemical weathering and physical erosion

Time-series sampling and analyses can reduce the uncertainty in estimating the rates of chemical weathering and physical erosion (Moon, Chamberlain, & Hilley, 2014; Zhong, Li, Tao, Yue, & Liu, 2017). The dissolved solute concentrations and carbon isotopes were modelled using the LoadRunner software package (Booth et al., 2007) of the

USGS LOADEST program (Runkel et al., 2004), and the results are shown in Figures 6a,b. Low concentrations occur in the high-flow season, while the highest concentrations occur in the low-flow season (Figure 6a,b). Most ions vary in a synchronal pattern, displaying similar and moderately chemostatic behaviour in response to the changing discharge. However, large quantities of surface water flow through the surface siliceous soil layers and regolith under high-flow conditions, resulting in high concentrations of Si in the river water (Gao et al., 2009).

A forward modelling method was employed to quantify the contribution of different sources of the cations in the river (Figure S1; Galy & France-Lanord, 1999; Han & Liu, 2004; Li et al., 2010; Rai et al., 2010; Xu & Liu, 2010), and TZ^+_{carb} and TZ^+_{sil} represent cations from the weathering of carbonate and silicate, respectively. A strong positive relationship was observed between the ratios of TZ^+_{carb}/TZ^+_{sil} and the discharge, indicating that TZ^+_{sil} has a higher sensitivity to discharge change than TZ^+_{carb} (Figure 7a). Similar trends were also demonstrated by climate-impacted global rivers, such as the Marsyandi (Tipper et al., 2006), the St. Lawrence (Szramek et al., 2007), the Danube (Szramek et al., 2007), the Rhone (Ollivier et al., 2010), the Wujiang (Zhong, Li, Tao, Ding, & Liu, 2017), the Minjiang (Zhong, Li, Tao, Yue, & Liu, 2017), and the Xijiang (Zhong et al., 2018).

The silicate weathering rate (SWR) was calculated using the Na^+ , K^+ , Ca^{2+} , Mg^{2+} , and SiO_2 concentrations of silicate weathering

sources, and the carbonate weathering rate (CWR) was estimated by the Ca^{2+} , Mg^{2+} , and HCO_3^- concentrations from carbonate dissolution by both sulphuric and carbonic acids, as described by Equations (S11) and (S12), respectively (Galy & France-Lanord, 1999; Han & Liu, 2004; Jiang et al., 2018; Xu & Liu, 2010). The SWR ranges from $1.1 \text{ t km}^{-2} \text{ year}^{-1}$ in the low-flow season to $44.9 \text{ t km}^{-2} \text{ year}^{-1}$ in the high-flow season, averaging $7.6 \text{ t km}^{-2} \text{ year}^{-1}$ (Table 1), which is much higher than that of the Seine ($1.2\text{--}2.6 \text{ t km}^{-2} \text{ year}^{-1}$, Roy et al., 1999) but lower than that of the Rhone ($14.4 \text{ t km}^{-2} \text{ year}^{-1}$, Ollivier et al., 2010). Meanwhile, the CWR ranges from $13.4 \text{ t km}^{-2} \text{ year}^{-1}$ in the low-flow season to $344.0 \text{ t km}^{-2} \text{ year}^{-1}$ in the high-flow season, averaging $69.7 \text{ t km}^{-2} \text{ year}^{-1}$ (Table 1), which is similar to that of the Seine (Roy et al., 1999), but lower than that of the Rhone ($89 \text{ t km}^{-2} \text{ year}^{-1}$, Ollivier et al., 2010). The CO_2 consumption flux of the Yu River is $8.7 \times 10^9 \text{ mol year}^{-1}$ and $50.7 \times 10^9 \text{ mol year}^{-1}$ for silicate weathering and carbonate weathering, respectively, which account for 0.1 and 0.4% of the global CO_2 consumption fluxes by silicate and carbonate weathering, respectively (Gaillardet et al., 1999).

Physical erosion is one of the most important geomorphic processes following which localised weathering occurs at high rates. Furthermore, the physical erosion rate significantly influences the reactive surface of the rock under climatic variability on a global scale (Galy & France-Lanord, 1999; Louvat & Allègre, 1997; Millot

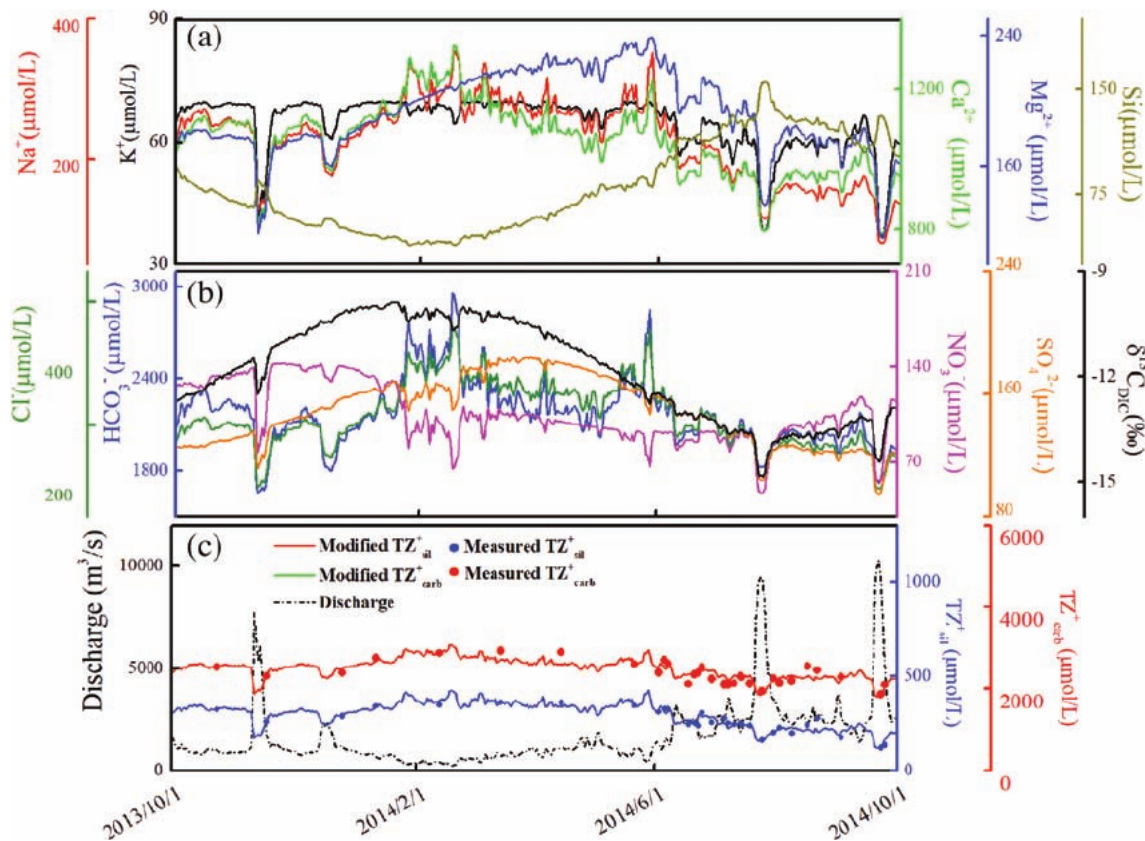


FIGURE 6 The modelled cation contents (a), anion contents and $\delta^{13}C_{DIC}$ (b), the modified and calculated TZ^+_{carb} and TZ^+_{sil} (c) for the Yu River in the hydrological year

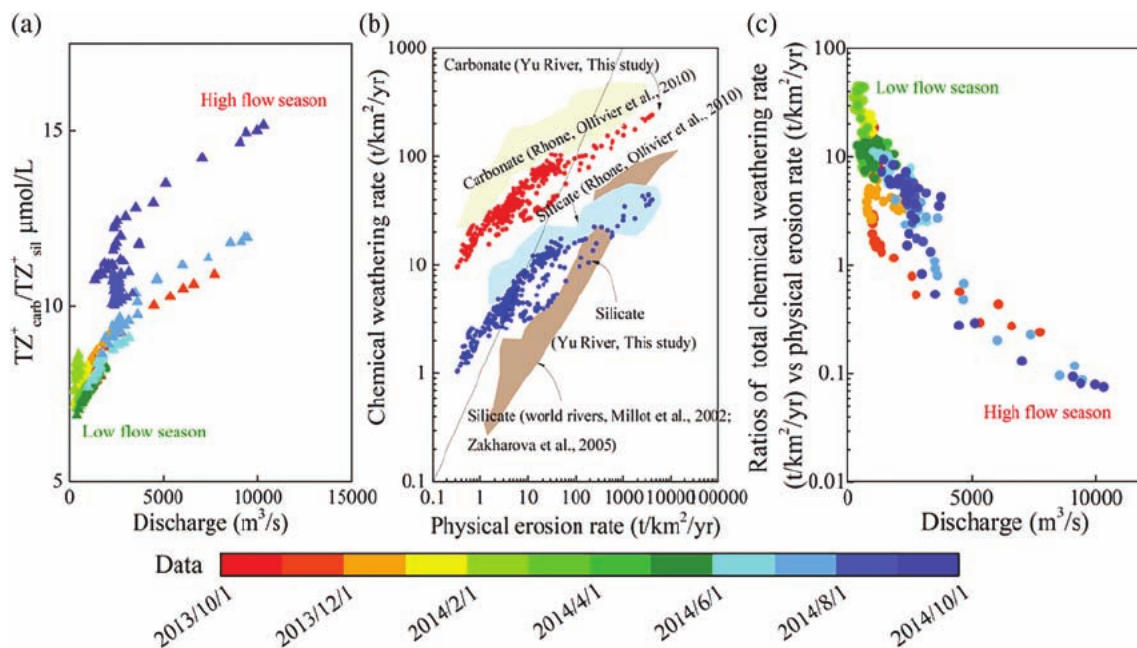


FIGURE 7 The relationships between TZ_{carb}^+/TZ_{sil}^+ ratios and discharge (a), chemical weathering rate and physical erosion rate (b), ratios of total chemical weathering versus physical erosion rate and discharge in the Yu River (c)

et al., 2002; Ollivier et al., 2010), implying that the supply of fresh unaltered minerals from mechanical erosion would alter the weathering rate (Ollivier et al., 2010). However, water chemistry is also affected by factors including discharge, temperature, and land cover, among others (Ollivier et al., 2010). Figure 7b shows the positive relationship between the chemical weathering rates and physical erosion rates that occur in the Yu River (Millot et al., 2002; Zakharova, Pokrovsky, Dupré, & Zaslavskaya, 2005). Globally, physical erosion rates and chemical weathering rates exhibit a synchronous trend (Figure 7b) because of the regulation of hydrological variability. There was a strong negative relationship between the ratio of the total weathering rate and the physical erosion rate in response to variability in discharge (Figure 7c). The physical erosion rates were found to increase in tens or even hundreds of times compared to those in the high-flow season, and their extent was greater than the total chemical weathering rates. The correlation of the physical erosion rates and chemical weathering rates can be attributed to the increasing intensity of erosion in response to high discharge promoted by monsoonal climate conditions. Hydrologic flushing further exposes reactive mineral surface area and, hence, accelerates rock weathering (Clow & Mast, 2010; Ollivier et al., 2010).

4.4 | Carbon dynamic and the control factors

$\delta^{13}C_{DIC}$ is a useful tool for tracing fluvial carbon sources and has a higher sensitivity than the riverine DIC content in response to discharge variability (Waldron, Scott, & Soulsby, 2007; Zhong et al., 2018). Figure 6b shows that heavy $\delta^{13}C_{DIC}$ values occur in low-flow conditions while light $\delta^{13}C_{DIC}$ values occur in high-flow

conditions, which is consistent with previous studies (Galy & France-Lanord, 1999; Hélie et al., 2002; Li et al., 2010; McClanahan et al., 2016; Schulte et al., 2011; Waldron et al., 2007; Zhong et al., 2018; Zhong, Li, Tao, Yue, & Liu, 2017). The normalised discharge (NQ) and normalised temperature (NT) are used to quantify the relative temporal discharge/temperature dynamics:

$$NQ = (Q_i - Q_{min}) / (Q_{max} - Q_{min}), \quad (3)$$

$$NT = (T_i - T_{min}) / (T_{max} - T_{min}), \quad (4)$$

where Q_i and T_i represent the respective instantaneous discharge rate and water temperature rate at the time i , and min and max represent the minimum and maximum values, respectively. There are negative relationships between $\delta^{13}C_{DIC}$ and both NQ and NT in the Yu River (Figure 8a,b), indicating that light $\delta^{13}C_{DIC}$ values are associated with high discharge and temperature conditions. Furthermore, discharge changes alter the fluid flow paths (Tipper et al., 2006), which would shift the $\delta^{13}C_{DIC}$ values by altering the mixing contribution of different sources (Lee & Krothe, 2001). In high-flow conditions, large amounts of $\delta^{13}C$ -depleted carbon, stored in the matrix porosity, are released into the river (Li et al., 2010). C_3 plants are dominant in the research area with an average $\delta^{13}C$ value of -27% (Li et al., 2008), and the $\delta^{13}C$ value of soil CO_2 is -22.6% , after considering the carbon isotope fractionation of 4.4% (Cerling et al., 1991; Clark & Fritz, 1997). In addition, high temperatures could encourage biological activity, resulting in strong photosynthesis/respiration, and soil organic material decomposition, which could cause larger amounts of soil-derived CO_2 to flush into the river (Li et al., 2010), resulting in more negative $\delta^{13}C_{DIC}$ values.

TABLE 1 The SWR, CWR, TWR, CO_{2sil}, CO_{2carb} and physical erosion rates for the Yu River in this study (during the hydrological year of October 2013 to September 2014) and previous studies

Location	Discharge (km ³ year ⁻¹)	SWR (t km ⁻² year ⁻¹)	CWR (t km ⁻² year ⁻¹)	TWR (t km ⁻² year ⁻¹)	FCO _{2sil} (10 ⁹ mol year ⁻¹)	RCO _{2sil} (10 ⁹ mol km ⁻² year ⁻¹)	FCO _{2carb} (10 ⁹ mol year ⁻¹)	RCO _{2carb} (10 ⁹ mol km ⁻² year ⁻¹)	Physical erosion (t km ⁻² year ⁻¹)	
Guijing	53.3	7.6	69.7	84.6	8.7	96.6	50.7	564.3	112	This study
Guijing	50.2	4.8 ± 0.3	70.1 ± 1.0	74.9 ± 1.3	4.5 ± 0.8	50 ± 10	56.1 ± 0.8	624 ± 9		Jiang et al., 2018
Guijing	50.2	6.48	80.2	87.4	8.3	91.2	75.4	830		Xu & Liu, 2010

Note: FCO_{2sil}, CO₂ consumption flux by silicate weathering; RCO_{2sil}, CO₂ consumption rate by silicate weathering; FCO_{2carb}, CO₂ consumption flux by carbonate weathering; RCO_{2carb}, CO₂ consumption rate by carbonate weathering.

Abbreviations: CWR, carbonate weathering rate; SWR, silicate weathering rate; TWR, total chemical weathering rate.

The difference between the measured and theoretical DIC values (from the theoretical dilution curve) is defined as ΔDIC (Zhong et al., 2018). DIC shows chemostatic behaviour in response to the increasing discharge, suggesting that large amounts of exogenous DIC are flushed into the river under high-flow conditions. δ¹³C_{DIC} slowly increases, then sharply decreases with increasing ΔDIC (Figure 8c). Meanwhile, in the low-flow season, due to low temperatures, weak soil respiration produces less CO₂ for replenishing the exogenous DIC. Therefore, relatively stable δ¹³C_{DIC} values were observed with increasing ΔDIC under the low-flow conditions (Figure 8c), indicating that carbon dynamics are mainly controlled by carbonate dissolution and precipitation processes in the low-flow season. In the high-flow season, a significantly negative relationship between ΔDIC and δ¹³C_{DIC} was observed, as shown in Figure 8c, indicating that large amounts of exogenous DIC, with δ¹³C-depleted values, flowed into the Yu River. Large amounts of organic carbon are also flushed into the river by physical erosion during flood events (Gao et al., 2009), which could be mineralised to DIC within several days (Ward et al., 2013). Therefore, carbonate weathering and biological CO₂ are responsible for riverine DIC temporal dynamics.

The mixing model *IsoSource* was employed to calculate the carbon sources based on the δ¹³C values of distinct DIC endmembers. According to previous studies in the research area (Li et al., 2008), the isotope values were taken to be 0‰ for carbonate carbon and -22.6‰ for biological carbon as end members. It has been demonstrated that rivers in the study catchment are generally supersaturated with respect to atmospheric CO₂, resulting in large CO₂ outgassing fluxes to the atmosphere (Yao et al., 2007). Hence, the kinetic fractionation of CO₂ outgassing is assumed to be -14.7%. The source contributions to riverine DIC can be calculated using:

$$\delta^{13}\text{C}_{\text{DIC}} = \delta^{13}\text{C}_{\text{carb}} \times a + \delta^{13}\text{C}_{\text{bio}} \times b - \delta^{13}\text{C}_{\text{out}} \times c, \quad (5)$$

$$a + b + c = 1, \quad (6)$$

where δ¹³C_{carb}, δ¹³C_{bio} and δ¹³C_{out} are the carbon isotopic values of carbonate (DIC_{carb}), biological carbon (DIC_{bio}), and CO₂ outgassing, respectively; *a* and *b* are the proportions of carbon from carbonate and biological carbon sources, respectively; and *c* is the proportion of carbon loss by CO₂ outgassing. Considering the occurrence of carbonate precipitation, the contribution of biological carbon would be underestimated.

Based on the calculation, DIC loss by CO₂ outgassing decreases from 8% in the low-flow conditions to 6% in the high-flow conditions, which could be because the water-gas exchange is lower in the high-flow season than that in the low-flow season (Figure 9a) (Doctor et al., 2008; McClanahan et al., 2016; Schulte et al., 2011; Zhang, Quay, & Wilbur, 1995). Moreover, the contribution of DIC_{carb} ranges from 38% in low-flow conditions to 30% in high-flow conditions, which could be due to the fast kinetics of carbonate dissolution. The contribution of DIC_{bio} increases from 54% in low-flow conditions to 64% in high-flow conditions, which presents a strong linear relationship with the discharge change,

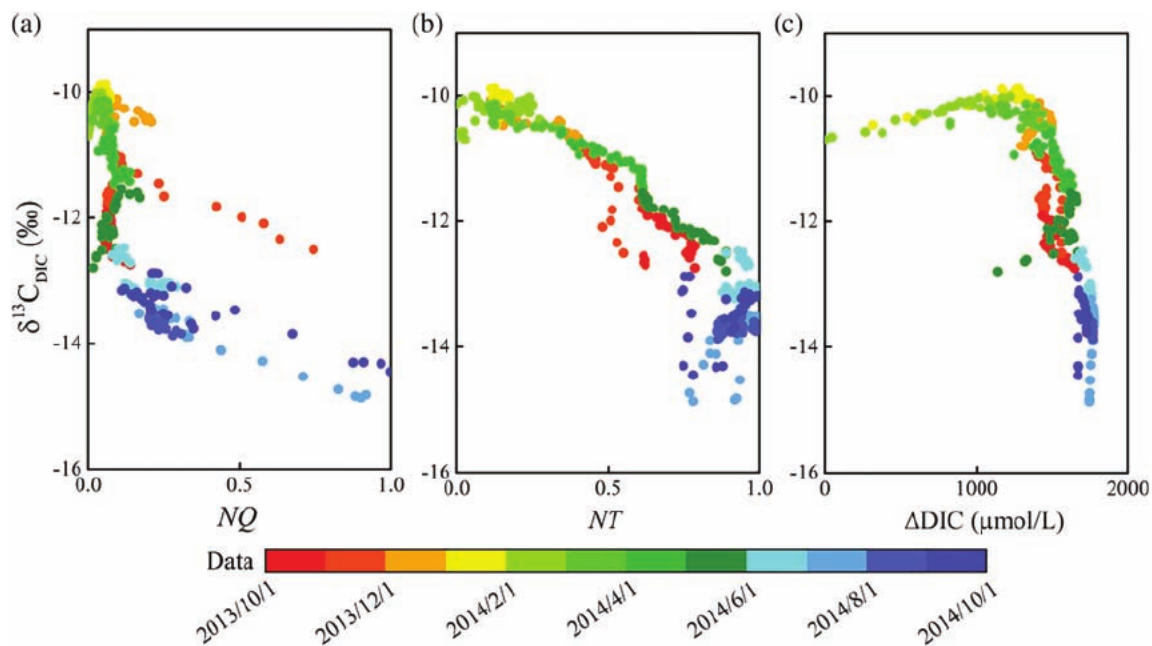
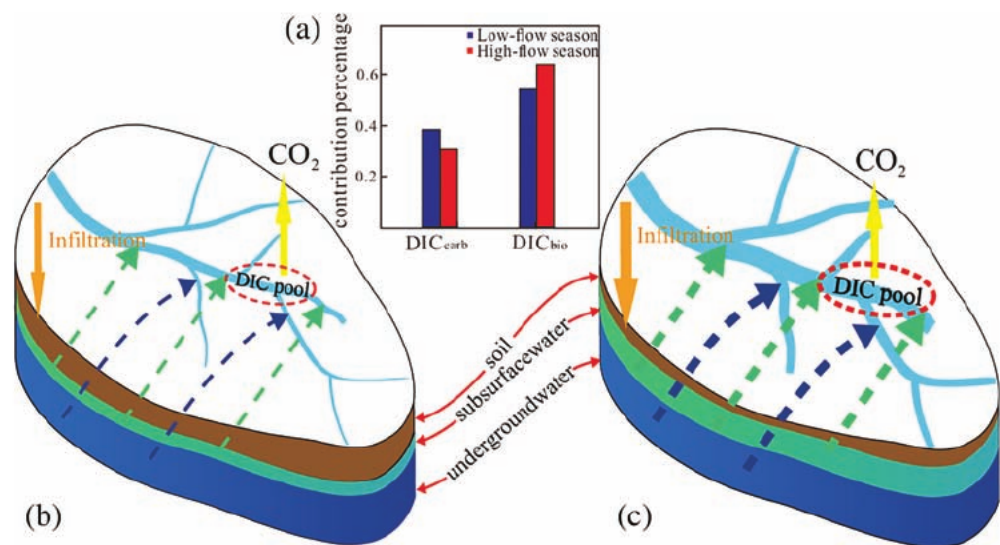


FIGURE 8 The relationships between $\delta^{13}\text{C}_{\text{DIC}}$ values versus NQ (normalized discharge) (a), NT (normalized temperature) (b) and ΔDIC (c) for Yu River in the hydrological year

FIGURE 9 The contribution proportion of DIC_{bio} and DIC_{carb} endmembers to riverine DIC in the high-flow season and in the low-flow season for the Yu River (a). The concept model for riverine DIC cycle in this study river in the low-flow season (b) and in the high-flow season (c)



indicating that DIC_{bio} is the dominant controller of the chemostatic behaviour of the total riverine DIC with increasing discharge, in line with previous studies (Li et al., 2010; Zhong, Li, Tao, Ding, & Liu, 2017). Therefore, rainwater infiltrates the soil and flushes excessive DIC_{bio} into the river, leading to an increase in DIC_{bio} in the high-flow season (Figure 9a). Although DIC concentrations show strong chemostatic behaviour in response to hydrological variability, the composition of DIC is markedly affected by changing climate conditions. Additional work is required to better delineate the isotope fractionation during CO_2 outgassing, which can influence DIC transportation and the global carbon cycle.

5 | CONCLUSIONS

This study investigated the biogeochemical processes of dissolved solutes and carbon dynamics under various hydrological conditions in a monsoonal river in South China. Carbonate weathering is the foremost contributor of dissolved solutes, showing stronger chemostatic behaviour than silicate weathering in the Yu River in response to hydrological changes. A strongly negative relationship was observed between the ratios of the total chemical weathering rate versus the physical erosion rate and the changing levels of discharge in this study. This correlation can be attributed to the increased erosion

intensity in response to the high discharge promoted by the monsoonal climate conditions. Under high-flow conditions, the near-chemostatic behaviour of carbonate weathering may be ascribed to the fast kinetics of carbonate dissolution.

Furthermore, under high-temperature conditions, the increase of photosynthesis and respiration would shift $\delta^{13}\text{C}_{\text{DIC}}$ to more negative values in the high-flow season than those in the low-flow season. *IsoSource* was used in this study to trace the carbon sources, demonstrating that biological carbon is the predominant controller of the riverine DIC. Therefore, the carbon isotopic compositions have a higher sensitivity than that of the DIC content in response to changing hydrological conditions. Additionally, time-series sampling and analyses in various climatic and geographic regions are needed, which could provide a better understanding of chemical weathering processes and riverine carbon dynamics resulting from global climate change.

ACKNOWLEDGMENTS

We would like to thank Prof. Rob M. Ellam for his valuable comments, which have markedly improved the scientific writing of this paper. This work was supported financially by the National Key R&D Program of China through Grant No. 2016YFA0601002, The National Natural Science Foundation of China (Grant Nos. 41571130072, 41861144026), the Guizhou Science and Technology Department Fund (Grant No. [2019]1043), Guizhou Education Department Fund (Grant No. [2018]161) and the scientific platform talent project of Guizhou University of Finance and Economics (Grant No. [2018] 5774-029).

CONFLICT OF INTEREST

The authors declare no potential conflict of interest.

DATA AVAILABILITY STATEMENT

The data that support the findings of this study are openly available in figshare at <http://doi.org/10.6084/m9.figshare.9730310>.

ORCID

Jing Liu  <https://orcid.org/0000-0002-1826-9361>

Jun Zhong  <https://orcid.org/0000-0003-2419-034X>

REFERENCES

- Ali, G., Wilson, H., Elliott, J., Penner, A., Haque, A., Ross, C., & Rabie, M. (2017). Phosphorus export dynamics and hydrobiogeochemical controls across gradients of scale, topography and human impact. *Hydrological Processes*, 31(18), 3130–3145. <https://doi.org/10.1002/hyp.11258>
- Amiotte Suchet, P., Probst, J.-L., & Ludwig, W. (2003). Worldwide distribution of continental rock lithology: Implications for the atmospheric/soil CO_2 uptake by continental weathering and alkalinity river transport to the oceans. *Global Biogeochemical Cycles*, 17(2), 1038. <https://doi.org/10.1029/2002gb001891>
- Booth, G., Raymond, P., & Oh, N.-H. (2007). LoadRunner. New Haven, CT. <http://environment.yale.edu/raymond/loadrunner>.
- Bouillon, S., Yambélé, A., Gillikin, D. P., Teodoru, C., Darchambeau, F., Lambert, T., & Borges, A. V. (2014). Contrasting biogeochemical characteristics of the Oubangui River and tributaries (Congo River basin). *Scientific Reports*, 4, 5402. <https://doi.org/10.1038/srep05402>
- Brunet, F., Dubois, K., Veizer, J., Nkoue Ndondo, G. R., Ndam Ngoupayou, J. R., Boeglin, J. L., & Probst, J. L. (2009). Terrestrial and fluvial carbon fluxes in a tropical watershed: Nyong basin, Cameroon. *Chemical Geology*, 265(3-4), 563–572. <https://doi.org/10.1016/j.chemgeo.2009.05.020>
- Cerling, T. E., Solomon, D. K., Quade, J., & Bowman, J. R. (1991). On the isotopic composition of carbon in soil carbon dioxide. *Geochimica et Cosmochimica Acta*, 55(11), 3403–3405. [https://doi.org/10.1016/0016-7037\(91\)90498-t](https://doi.org/10.1016/0016-7037(91)90498-t)
- Clark, I., & Fritz, P. (1997). *Environmental isotopes in hydrogeology*. Boca Raton, FL: Lewis Publishers.
- Clow, D. W., & Mast, M. A. (2010). Mechanisms for chemostatic behavior in catchments: Implications for CO_2 consumption by mineral weathering. *Chemical Geology*, 269(1-2), 40–51. <https://doi.org/10.1016/j.chemgeo.2009.09.014>
- Diamond, J. S., & Cohen, M. J. (2018). Complex patterns of catchment solute-discharge relationships for coastal plain rivers. *Hydrological Processes*, 32(3), 388–401. <https://doi.org/10.1002/hyp.11424>
- Doctor, D. H., Kendall, C., Sebestyen, S. D., Shanley, J. B., Ohte, N., & Boyer, E. W. (2008). Carbon isotope fractionation of dissolved inorganic carbon (DIC) due to outgassing of carbon dioxide from a headwater stream. *Hydrological Processes*, 22(14), 2410–2423. <https://doi.org/10.1002/hyp.6833>
- Dubois, K. D., Lee, D., & Veizer, J. (2010). Isotopic constraints on alkalinity, dissolved organic carbon, and atmospheric carbon dioxide fluxes in the Mississippi River. *Journal of Geophysical Research: Biogeosciences*, 115(G2), 02018. <https://doi.org/10.1029/2009jg001102>
- Gaillardet, J., Dupré, B., Louvat, P., & Allègre, C. J. (1999). Global silicate weathering and CO_2 consumption rates deduced from the chemistry of rivers. *Chemical Geology*, 159, 3–30. [https://doi.org/10.1016/S0009-2541\(99\)00031-5](https://doi.org/10.1016/S0009-2541(99)00031-5)
- Galy, A., & France-Lanord, C. (1999). Weathering processes in the Ganges-Brahmaputra basin and the riverine alkalinity budget. *Chemical Geology*, 159(1-4), 31–60. [https://doi.org/10.1016/S0009-2541\(99\)00033-9](https://doi.org/10.1016/S0009-2541(99)00033-9)
- Gao, Q. Z., Tao, Z., Huang, X. K., Nan, L., Yu, K. F., & Wang, Z. G. (2009). Chemical weathering and CO_2 consumption in the Xijiang River basin, South China. *Geomorphology*, 106(3-4), 324–332. <https://doi.org/10.1016/j.geomorph.2008.11.010>
- Gareis, J. A., & Lesack, L. F. (2017). Fluxes of particulates and nutrients during hydrologically defined seasonal periods in an ice-affected great Arctic river, the Mackenzie. *Water Resources Research*, 53(7), 6109–6132. <https://doi.org/10.1002/2017WR020623>
- Geological Bureau of Guangxi Zhuang Autonomous Region. (1985). *Regional geological archive of Guangxi Zhuang autonomous region*. Beijing, China: Geological Publishing House. (in Chinese).
- Godsey, S. E., Kirchner, J. W., & Clow, D. W. (2009). Concentration-discharge relationships reflect chemostatic characteristics of US catchments. *Hydrological Processes*, 23(13), 1844–1864. <https://doi.org/10.1002/hyp.7315>
- Gwenzi, W., Chinyama, S. R., & Togarepi, S. (2017). Concentration-discharge patterns in a small urban headwater stream in a seasonally dry water-limited tropical environment. *Journal of Hydrology*, 550, 12–25. <https://doi.org/10.1016/j.jhydrol.2017.04.029>
- Han, G. L., & Liu, C.-Q. (2004). Water geochemistry controlled by carbonate dissolution: A study of the river waters draining karst-dominated terrain, Guizhou Province, China. *Chemical Geology*, 204(1-2), 1–21. <https://doi.org/10.1016/j.chemgeo.2003.09.009>
- Hélie, J.-F., Hillaire-Marcel, C., & Rondeau, B. (2002). Seasonal changes in the sources and fluxes of dissolved inorganic carbon through the St. Lawrence River—isotopic and chemical constraint. *Chemical Geology*, 186, 117–138. [https://doi.org/10.1016/S0009-2541\(01\)00417-X](https://doi.org/10.1016/S0009-2541(01)00417-X)

- Jiang, H., Liu, W., Zhao, T., Sun, H., & Xu, Z. (2018). Water geochemistry of rivers draining karst-dominated regions, Guangxi province, South China: Implications for chemical weathering and role of sulfuric acid. *Journal of Asian Earth Science*, *163*, 152–162. <https://doi.org/10.1016/j.jseas.2018.05.017>
- Kim, H., Dietrich, W. E., Thurnhoffer, B. M., Bishop, J. K. B., & Fung, I. Y. (2017). Controls on solute concentration-discharge relationships revealed by simultaneous hydrochemistry observations of hillslope runoff and stream flow: The importance of critical zone structure. *Water Resources Research*, *53*(2), 1424–1443. <https://doi.org/10.1002/2016wr019722>
- Koger, J. M., Newman, B. D., & Goering, T. J. (2018). Chemostatic behaviour of major ions and contaminants in a semiarid spring and stream system near Los Alamos, NM, USA. *Hydrological Processes*, *32*(11), 1799–1716. <https://doi.org/10.1002/hyp.11624>
- Krishna, M. S., Viswanadham, R., Prasad, M. H. K., Kumari, V. R., & Sarma, V. V. S. S. (2018). Export fluxes of dissolved inorganic carbon to the northern Indian Ocean from the Indian monsoonal rivers. *Biogeosciences Discussions*, *16*(2), 505–519. <https://doi.org/10.5194/bg-2018-4>
- Lee, E. S., & Krothe, N. C. (2001). A four-component mixing model for water in a karst terrain in south-Central Indiana, USA. Using solute concentration and stable isotopes as tracers. *Chemical Geology*, *179*, 129–143. [https://doi.org/10.1016/S0009-2541\(01\)00319-9](https://doi.org/10.1016/S0009-2541(01)00319-9)
- Li, S.-L., Calmels, D., Han, G., Gaillardet, J., & Liu, C.-Q. (2008). Sulfuric acid as an agent of carbonate weathering constrained by $\delta^{13}\text{C}_{\text{DIC}}$: Examples from Southwest China. *Earth and Planetary Science Letters*, *270*(3-4), 189–199. <https://doi.org/10.1016/j.epsl.2008.02.039>
- Li, S.-L., Liu, C.-Q., Li, J., Lang, Y.-C., Ding, H., & Li, L. (2010). Geochemistry of dissolved inorganic carbon and carbonate weathering in a small typical karstic catchment of Southwest China: Isotopic and chemical constraints. *Chemical Geology*, *277*(3-4), 301–309. <https://doi.org/10.1016/j.chemgeo.2010.08.013>
- Li, S. Y., & Bush, R. T. (2015). Changing fluxes of carbon and other solutes from the Mekong River. *Scientific Reports*, *5*, 16005. <https://doi.org/10.1038/srep16005>
- Liu, J., Li, S.-L., Zhong, J., Zhu, X. T., Guo, Q. J., Lang, Y. C., & Han, X. K. (2017). Sulfate sources constrained by sulfur and oxygen isotopic compositions in the upper reaches of the Xijiang River, China. *Acta Geochimica*, *36*(4), 611–618. <https://doi.org/10.1007/s11631-017-0175-1>
- Louvat, P., & Allègre, C. J. (1997). Present denudation rates on the Island of Réunion determined by river geochemistry: Basalt weathering and mass budget between chemical and mechanical erosions. *Geochimica et Cosmochimica Acta*, *61*, 3645–3661. [https://doi.org/10.1016/S0016-7037\(97\)00180-4](https://doi.org/10.1016/S0016-7037(97)00180-4)
- Maher, K., & Chamberlain, C. P. (2014). Hydrologic regulation of chemical weathering and the geologic carbon cycle. *Science*, *343*(6178), 1502–1504. <https://doi.org/10.1126/science.1250770>
- McClanahan, K., Polk, J., Groves, C., Osterhoudt, L., & Grubbs, S. (2016). Dissolved inorganic carbon sourcing using $\delta^{13}\text{C}_{\text{DIC}}$ from a karst influenced river system. *Earth Surface Processes and Landforms*, *41*(3), 392–405. <https://doi.org/10.1002/esp.3856>
- Millot, R., Gaillardet, J., Dupré, B., & Allègre, C. J. (2002). The global control of silicate weathering rates and the coupling with physical erosion: New insights from rivers of the Canadian shield. *Earth and Planetary Science Letters*, *196*, 83–98. [https://doi.org/10.1016/S0012-821X\(01\)00599-4](https://doi.org/10.1016/S0012-821X(01)00599-4)
- Moon, S., Chamberlain, C. P., & Hillel, G. E. (2014). New estimates of silicate weathering rates and their uncertainties in global rivers. *Geochimica et Cosmochimica Acta*, *134*, 257–274. <https://doi.org/10.1016/j.gca.2014.02.033>
- Musolff, A., Schmidt, C., Selle, B., & Fleckenstein, J. H. (2015). Catchment controls on solute export. *Advances in Water Resources*, *86*, 133–146. <https://doi.org/10.1016/j.advwatres.2015.09.026>
- Ollivier, P., Hamelin, B., & Radakovitch, O. (2010). Seasonal variations of physical and chemical erosion: A three-year survey of the Rhone River (France). *Geochimica et Cosmochimica Acta*, *74*(3), 907–927. <https://doi.org/10.1016/j.gca.2009.10.037>
- Pearl River Conservancy Committee (PRCC). (2013). *The hydrological year-books of Pearl River (in Chinese)*. Beijing, China: PRCC. (in Chinese).
- Rai, S. K., Singh, S. K., & Krishnaswami, S. (2010). Chemical weathering in the plain and peninsular sub-basins of the ganga: Impact on major ion chemistry and elemental fluxes. *Geochimica et Cosmochimica Acta*, *74*(8), 2340–2355. <https://doi.org/10.1016/j.gca.2010.01.008>
- Raymond, P. A., & Cole, J. J. (2003). Increase in the export of alkalinity from North America's largest river. *Science*, *301*(5629), 88–91. <https://doi.org/10.1126/science.1083788>
- Rose, L. A., Karwan, D. L., & Godsey, S. E. (2018). Concentration-discharge relationships describe solute and sediment mobilization, reaction, and transport at event and longer timescales. *Hydrological Processes*, *32*(18), 2829–2844. <https://doi.org/10.1002/hyp.13235>
- Roy, S., Gaillardet, J., & Allegre, C. J. (1999). Geochemistry of dissolved and suspended loads of the seine river, France: Anthropogenic impact, carbonate and silicate weathering. *Geochimica et Cosmochimica Acta*, *63*(9), 1277–1292. [https://doi.org/10.1016/S0016-7037\(99\)00099-x](https://doi.org/10.1016/S0016-7037(99)00099-x)
- Rue, G. P., Rock, N. D., Gabor, R. S., Pitlick, J., Tfaily, M., & McKnight, D. M. (2017). Concentration-discharge relationships during an extreme event: Contrasting behavior of solutes and changes to chemical quality of dissolved organic material in the Boulder Creek watershed during the September 2013 flood. *Water Resources Research*, *53*(7), 5276–5297. <https://doi.org/10.1002/2016wr019708>
- Runkel, R.L., Crawford, C.G., & Cohn, T.A. (2004). Load Estimator (LOADEST): A FORTRAN Program for Estimating Constituent Loads in Streams and Rivers, U.S. Geol. Surv. Tech. and Meth., book 4, chap. A5, p. 69, U.S. Geol. Surv., Denver, Colo.
- Schulte, P., van Geldern, R., Freitag, H., Karim, A., Négrel, P., Petelet-Giraud, E., ... Barth, J. A. C. (2011). Applications of stable water and carbon isotopes in watershed research: Weathering, carbon cycling, and water balances. *Earth-Science Reviews*, *109*(1-2), 20–31. <https://doi.org/10.1016/j.earscirev.2011.07.003>
- Singley, J. G., Wlostowski, A. N., Bergstrom, A. J., Sokol, E. R., Torrens, C. L., Jaros, C., ... Gooseff, M. N. (2017). Characterizing hyporheic exchange processes using high-frequency electrical conductivity-discharge relationships on subhourly to interannual timescales. *Water Resources Research*, *53*(5), 4124–4141. <https://doi.org/10.1002/2016wr019739>
- Szramek, K., McIntosh, J. C., Williams, E. L., Kanduc, T., Ogrinc, N., & Walter, L. M. (2007). Relative weathering intensity of calcite versus dolomite in carbonate-bearing temperate zone watersheds: Carbonate geochemistry and fluxes from catchments within the St. Lawrence and Danube river basins. *Geochemistry Geophysics Geosystems*, *8*(4), 1–26. <https://doi.org/10.1029/2006gc001337>
- Thompson, S. E., Basu, N. B., Lascurain, J., Aubeneau, A., & Rao, P. S. C. (2011). Relative dominance of hydrologic versus biogeochemical factors on solute export across impact gradients. *Water Resources Research*, *47*(10), W00J05.1–W00J05.20. <https://doi.org/10.1029/2010wr009605>
- Tipper, E. T., Bickle, M. J., Galy, A., West, A. J., Pomiès, C., & Chapman, H. J. (2006). The short term climatic sensitivity of carbonate and silicate weathering fluxes: Insight from seasonal variations in river chemistry. *Geochimica et Cosmochimica Acta*, *70*(11), 2737–2754. <https://doi.org/10.1016/j.gca.2006.03.005>
- Tobias, C., & Böhlke, J. K. (2011). Biological and geochemical controls on diel dissolved inorganic carbon cycling in a low-order agricultural stream: Implications for reach scales and beyond. *Chemical Geology*, *283*(1-2), 18–30. <https://doi.org/10.1016/j.chemgeo.2010.12.012>

- Torres, M. A., West, A. J., & Clark, K. E. (2015). Geomorphic regime modulates hydrologic control of chemical weathering in the Andes–Amazon. *Geochimica et Cosmochimica Acta*, 166, 105–128. <https://doi.org/10.1016/j.gca.2015.06.007>
- Waldron, S., Scott, E. M., & Soulsby, C. (2007). Stable isotope analysis reveals lower-Order River dissolved inorganic carbon pools are highly dynamic. *Environmental Science & Technology*, 41, 6156–6162. <https://doi.org/10.1021/es0706089>
- Ward, N. D., Keil, R. G., Medeiros, P. M., Brito, D. C., Cunha, A. C., Dittmar, T., ... Richey, J. E. (2013). Degradation of terrestrially derived macromolecules in the Amazon River. *Nature Geoscience*, 6(7), 530–533. <https://doi.org/10.1038/ngeo1817>
- Xu, Z. F., & Liu, C.-Q. (2010). Water geochemistry of the Xijiang basin rivers, South China: Chemical weathering and CO₂ consumption. *Applied Geochemistry*, 25(10), 1603–1614. <https://doi.org/10.1016/j.apgeochem.2010.08.012>
- Yao, G., Gao, Q., Wang, Z., Huang, X., He, T., Zhang, Y., ... Ding, J. (2007). Dynamics of CO₂ partial pressure and CO₂ outgassing in the lower reaches of the Xijiang River, a subtropical monsoon river in China. *Science of the Total Environment*, 376(1-3), 255–266. <https://doi.org/10.1016/j.scitotenv.2007.01.080>
- Yuan, D. (1991). *Karst of China*. Beijing, China: Geological Publishing House. (in Chinese).
- Zakharova, E. A., Pokrovsky, O. S., Dupré, B., & Zaslavskaya, M. B. (2005). Chemical weathering of silicate rocks in Aldan shield and Baikal uplift: Insights from long-term seasonal measurements of solute fluxes in rivers. *Chemical Geology*, 214(3-4), 223–248. <https://doi.org/10.1016/j.chemgeo.2004.10.003>
- Zhang, J., Quay, P. D., & Wilbur, D. O. (1995). Carbon isotope fractionation during gas–water exchange and dissolution of CO₂. *Geochimica et Cosmochimica Acta*, 59(1), 107–114. [https://doi.org/10.1016/0016-7037\(95\)91550-DGet](https://doi.org/10.1016/0016-7037(95)91550-DGet)
- Zhong, J., Li, S.-L., Liu, J., Ding, H., Sun, X. L., Xu, S., ... Liu, C.-Q. (2018). Climate variability controls on CO₂ consumption fluxes and carbon dynamics for monsoonal rivers: Evidence from Xijiang River, Southwest China. *Journal of Geophysical Research: Biogeosciences*, 123(8), 2553–2567. <https://doi.org/10.1029/2018jg004439>
- Zhong, J., Li, S.-L., Tao, F., Ding, H., & Liu, J. (2017). Impacts of hydrologic variations on chemical weathering and solute sources in the Min River basin, Himalayan-Tibetan region. *Environmental Science and Pollution Research*, 24(23), 19126–19137. <https://doi.org/10.1007/s11356-017-9584-2>
- Zhong, J., Li, S.-L., Tao, F., Yue, F., & Liu, C. Q. (2017). Sensitivity of chemical weathering and dissolved carbon dynamics to hydrological conditions in a typical karst river. *Scientific Reports*, 7, 42944. <https://doi.org/10.1038/srep42944>

SUPPORTING INFORMATION

Additional supporting information may be found online in the Supporting Information section at the end of this article.

How to cite this article: Liu J, Zhong J, Ding H, et al. Hydrological regulation of chemical weathering and dissolved inorganic carbon biogeochemical processes in a monsoonal river. *Hydrological Processes*. 2020;34:2780–2792. <https://doi.org/10.1002/hyp.13763>